Journal of Materials Chemistry A

Improved thermal and oxidation stability of bis(triethoxysilyl)ethane (BTESE)-derived membranes, and their gas-permeation properties

Journal:	*Journal of Materials Chemistry A*
Manuscript ID	TA-ART-08-2018-007572.R3
Article Type:	Paper
Date Submitted by the Author:	22-Oct-2018
Complete List of Authors:	Yu , Xin; Hiroshima University Kanezashi, Masakoto; Hiroshima University, Department of Chemical Engineering Nagasawa, Hiroki; Hiroshima University, Department of Chemical Engineering Tsuru, Toshinori; Hiroshima University, Department of Chemical Engineering

Bis(triethoxysilyl)ethane:

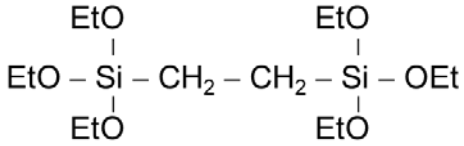

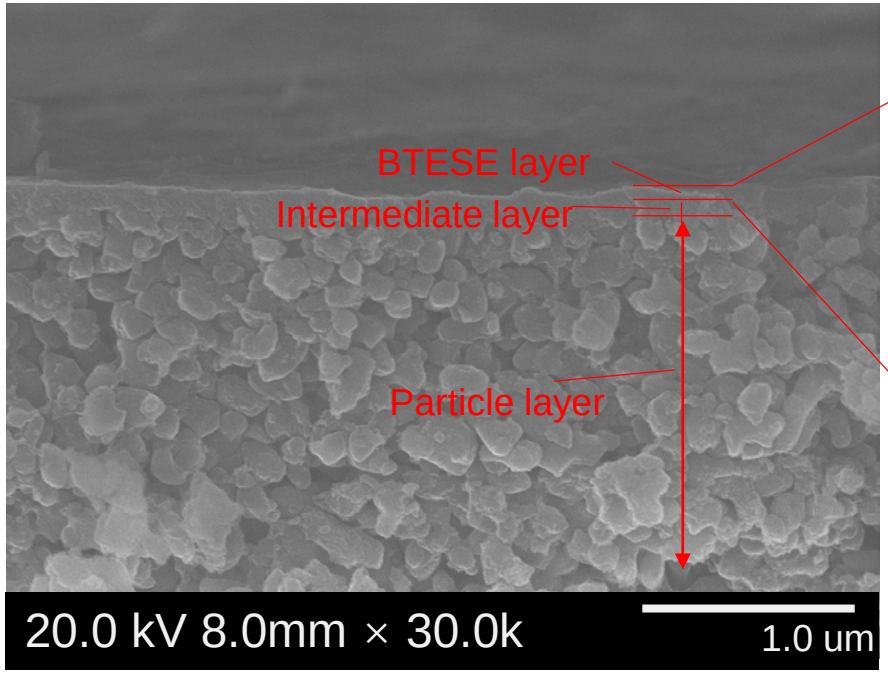

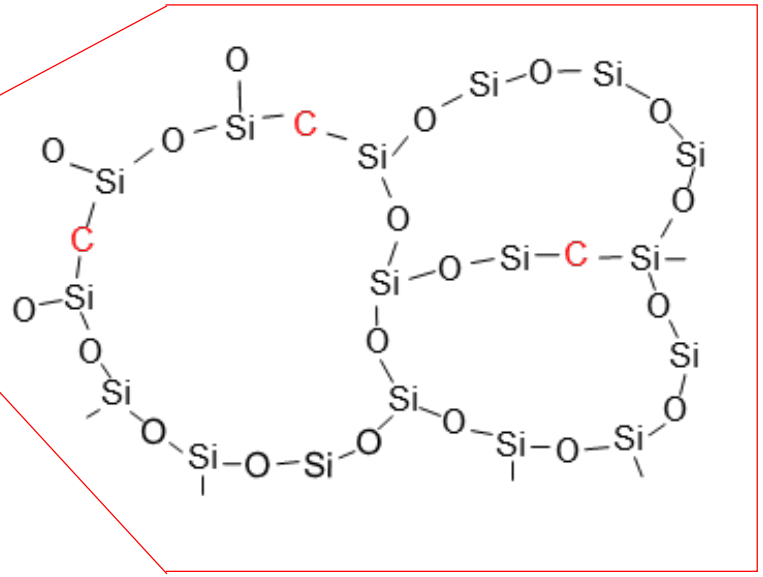

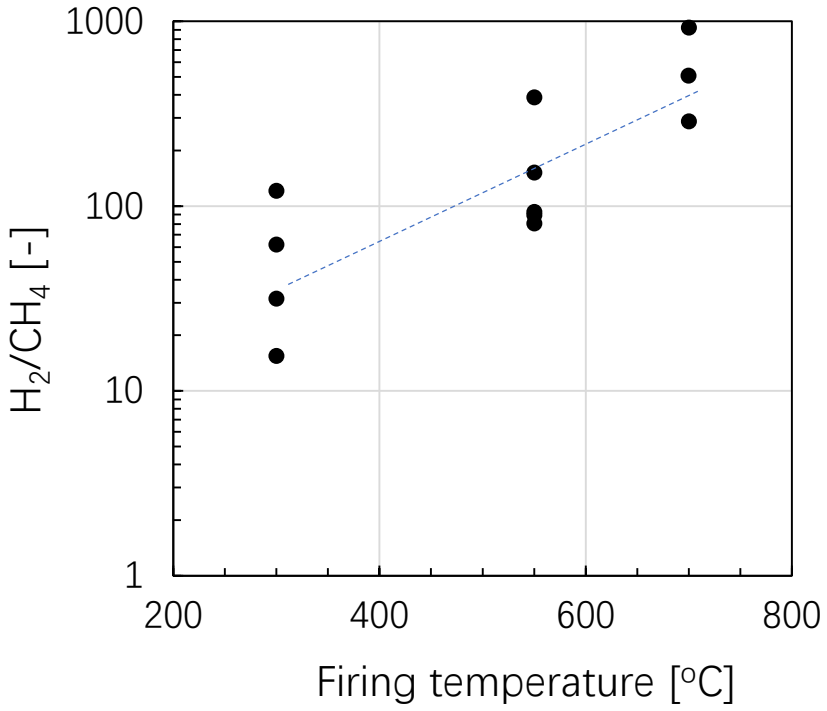

Selectivity increased with firing temperatures

Journal Name

ARTICLE

Improved thermal and oxidation stability of bis(triethoxysilyl)ethane (BTESE)-derived membranes, and their gas-permeation properties

Xin Yu, Hiroki Nagasawa, Masakoto Kanezashi, and Toshinori Tsuru*

Received 00th January 20xx,
Accepted 00th January 20xx

DOI: 10.1039/x0xx00000x

www.rsc.org/

The conventional method used to fabricate bis(triethoxysilyl)ethane (BTESE)-derived organosilica membranes begins with a coating of BTESE-derived sols that is then fired at temperatures that do not exceed 300 °C, because the organic linking ethane groups start to thermally decompose at temperatures higher than 300 °C. In the present study, however, thermal stability of BTESE membranes was further enhanced by firing at much higher temperatures (550–700 °C), which promises to enable future applications such as H_2 purification at high temperatures and gas separation under an oxidizing atmosphere. The selectivity of 700 °C-fired membranes for H_2/CH_4 was as high as 100 with H_2 permeance of approximately 10^{-6} mol/(m^2 s Pa). Moreover, even after heat treatment at 550 °C under N_2 and then under air, BTESE-derived membranes prepared at 550 °C showed high selectivity values of approximately 100 and 2000 for H_2/CH_4 and H_2/CF_4, respectively. By comparison, the selectivities for H_2/CH_4 and H_2/CF_4 of membranes prepared at 300 °C were approximately 30 and 200, respectively. The BTESE powders were characterized by FT-IR, N_2 adsorption, Electro-Probe Microanalyzer (EPMA), and TGA. The large carbon/silicon ratio and residual weight for powders with multiple heat treatments under N_2 and then under air, suggested that high-temperature treatment under N_2 increased the thermal stability and oxidizing resistance. These results showed that calcination temperatures, atmosphere, and heat treatment are the key factors influencing the thermal and oxidation stability of these BTESE membranes.

Introduction

Membrane separation has become an effective technology over the past several decades,[1] since an energy-efficient, easy and compact process can be used to separate mixtures in either the gas or liquid phase. Promising applications include energy-related separations and purifications such as H_2 purification under high temperatures in a catalytic membrane reactor,[2, 3] CH_4 purification of natural gas,[4] and CO_2 capture to arrest global warming.[5, 6] Various types of membranes prepared from inorganic materials such as zeolites, MOFs, carbon, silica, and hybrid materials have been explored for gas separation.[1, 7]

Amorphous silica membranes, which are typically prepared from tetraethoxysilane (TEOS),[8] have been extensively investigated for gas separation at high temperatures due to a level of thermal stability up to 1000 °C. Generally, silica membranes show high permselectivity at high temperatures; for example, He and H_2 permeance of 8.6×10^{-7} and 5.5×10^{-7} mol/(m^2 s Pa) with He/CH_4 and H_2/CH_4 permeance ratios of 2350 and 1500 at 500 °C, respectively, were reported and the H_2/N_2 permeance ratio was above 100 even after heat-treatment at 750 °C.[8] Generally, silica membranes have a microporous structure with an average pore size of 0.34 nm, which allows them to separate gas molecules via molecular sieving with extremely high levels of H_2 selectivity over other gases such as N_2 and over hydrocarbons such as CH_4 and propane.[8-10] The low stability of the silica structure in water vapor under hydrothermal conditions, however, is a disadvantage that prevents industrialization on a large scale.[11-13]

Recently, bis(triethoxysilyl)ethane (BTESE)-derived organosilica, which has CH_2CH_2 linking units between two silicon atoms, has been proposed for use in pervaporation[14] and gas separation.[15] Due to the incorporation of organic linking units, the pore sizes of BTESE membranes were successfully controlled to obtain a structure that was looser than that of TEOS-derived silica membranes prepared by the sol-gel method. In addition, the hydrothermal stability was also increased due to ethane hydrophobicity. These excellent properties have allowed a wider range of applications for BTESE membranes, which includes gas separations[16] such as H_2 purification,[11, 17-19] CO_2 removal from CH_4,[20-22] and use in membrane reactors.[2, 18, 23, 24] BTESE-derived membranes have also returned excellent performances in pervaporation dehydrations such as in IPA/H_2O,[25] reverse osmosis,[26] and vapor permeation[27, 28] due to a high level of hydrothermal stability.

Generally, the preparation of BTESE membranes includes two processes: sol preparation and gel calcination. The ethoxy groups of BTESE are hydrolyzed to form silanol groups, followed by condensation to form siloxane bridges. BTESE-derived membranes are prepared by coating the polymeric sols onto nanoporous substrates and firing. The H_2O/BTESE ratio in preparation of BTESE-derived sols is a significant factor; with an increase in the H_2O/BTESE molar ratio, the ethoxy groups of BTESE become more hydrolyzed and the number of silanol groups is increased, which is followed by increased densification of the networks and a resultant higher level of selectivity for BTESE-derived membranes.[18] In addition, the acid

Department of Chemical Engineering, Graduate School of Engineering, Hiroshima University. 1-4-1 Kagami-yama, Higashi-Hiroshima 739-8527, Japan
tsuru@hiroshima-u.ac.jp

Electronic Supplementary Information (ESI) available: [details of any supplementary information available should be included here]. See DOI: 10.1039/x0xx00000x

ratio, which is defined as the molar ratio of acid to BTESE, also plays an important role in controlling the hydrolysis and condensation ratio during the sol preparation.[21, 29-31] In our previous work, larger-sized sols prepared via the pH-swing method (acid→alkali→acid) were prevented from penetrating substrates, so that the pH-swing membranes showed high H_2 permeance without a loss of selectivity. Moreover, we found the thermal stability of pH-swing membranes was increased due to an increase in the cross-linking to form thermally stable siloxane bonds.[30] In addition, pore size and hydrophobicity/hydrophilicity were successfully controlled by processing parameters such as the firing temperature,[32, 33] atmosphere,[34] or membrane post-processing such as HCl treatment[35, 36] in attempts to improve the permeation properties.

BTESE-derived membranes have larger pores than TEOS-derived versions due to the linking units,[15] which allows them to separate H_2 from large sized hydrocarbons. One of the potential applications of separation is H_2 purification at high temperatures from C_3H_6, which is produced by catalytic dehydrogenation of C_3H_8 at temperatures higher than 580 °C.[37] But the thermal stability of BTESE membranes has remained unclear, because BTESE-derived membranes are usually prepared and used at temperatures lower than 300 °C due to decomposition of the organic linking units at high temperatures.[38] Qi et al. prepared BTESE membranes under firing temperatures higher than 400 °C and under different heating rates.[33] In that study, the organic linking groups in networks were sensitive to calcination conditions. For example, BTESE membranes fired at 400 and 600 °C showed low and high levels of cross-linking, respectively. BTESE membranes calcined at 600 °C demonstrated expeditious calcination that resulted in a high degree of cross-linking in a network that contained a high content of organic bridge groups. In these studies, BTESE membranes showed a H_2/CO_2 selectivity of 36 when measured at 200 °C under single-gas systems, which was increased with an increase in the firing temperatures of the membranes. However, the development of BTESE-derived membranes with thermal/ oxidation stability at high temperatures (500−600 °C) and high gas selectivity remains a challenge.

The main objective of the present study was to explore the possibility of improving the stability of BTESE-derived membranes at high temperatures under an oxidizing atmosphere. BTESE-derived sols were prepared via the pH-swing method, and membranes were prepared by coating BTESE sols and firing at 300, 550 and 700 °C under N_2. The BTESE powders were prepared in pre-treatments that ranged from 300 to 800 °C under N_2 with subsequent firing under air at 600 °C and analysis by TG, FT-IR, N_2 adsorption, and EPMA. The membrane performances were measured and compared via single-gas permeation. Time courses of permeance at high temperatures under N_2 and air were evaluated to better explain the thermal stability and oxidative resistance of BTESE membranes. The trade-offs of H_2 permeance and H_2/gas (He, N_2, CH_4) permeance ratios were summarized to discuss the properties of membranes prepared at high temperatures.

The present work is the first to describe how membranes that are defect-free, highly selective (H_2/CH_4>100), and with high levels of H_2 permeance (>10^{-6} mol/(m^2 s Pa)) can be prepared by firing at high temperatures. In addition, the superior thermal and oxidation stability of BTESE membranes prepared at 550 and 700 °C was confirmed via the time courses of permeance at high temperatures under N_2 and air, which holds promise for applications to gas separation under an O_2 atmosphere at high temperatures.

Experimental

Preparation of pH-swing BTESE sols

Samples of 1, 2-bis (triethoxysilyl) ethane (BTESE) and ethanol were purchased from Gelest Inc. and Sigma-Aldrich and were used as the precursor and solvent, respectively, without further purification. BTESE-derived acid and pH-swing sols were prepared via the hydrolysis and condensation of BTESE in ethanol according to our previous paper that describes the preparation procedure.[30] Briefly, BTESE was mixed with ethanol, water, and HCl as catalysts in molar ratios of BTESE/HCl/H_2O=1/0.01/240, and the weight %s of the precursors were adjusted to 5% via the use of ethanol as a solvent. BTESE-derived sols were prepared by a pH-swing method as follows. First, BTESE was hydrolyzed and condensed with water and hydrochloric acid at 50 °C for 1 h, then the pH value of the sols was changed from 2 to 9 by adding a specific amount of NH_3 and agitating for several minutes, followed by the addition of HCl to return the pH to approximately 2 at 25 °C.

Characterization of pH-swing BTESE gels

BTESE-derived powders were prepared by drying BTESE-derived sols which were then finely ground in a mortar. Thermogravimetric analysis (TG) was provided by TG-MASS (TG-DTA-410s, Rigaku Co). He and He/O_2 mixed gas (He: 80 mol%, O_2: 20 mol%) were used as a carrier gas, and the temperature was increased at a ramping rate of 5 °C/min. The residual weight of the samples was normalized at 250 °C to eliminate the influence of NH_4Cl.[30] BTESE powders fired at 100, 200, 300, 550, and 700 °C under N_2 (referred to here as P100, P200, P300, P550 and P700, respectively) were investigated via ATR-FTIR (FT/IR-4100, Jasco, Japan) using an MCT detector cooled with liquid nitrogen. Measurements within a recorded in the range of 4000−500 cm^{-1} were recorded at a resolution of 4 cm^{-1}. The adsorption isotherms of N_2 for P300, P550 and P700 were measured at 77 K (BELMAX, BEL Japan INC) after the samples were degassed under vacuum at 200 °C for more than 10 h. An electron probe micro-analyzer (EPMA) provided data for wavelength-dispersive X-ray analysis (EPMA JXA-8200, Rigaku Co., Japan).

Preparation of BTESE-derived membranes

BTESE-derived membranes were prepared as reported elsewhere.[18, 30, 31] Porous α-alumina tubes (porosity: 50%, inner and outer diameter of 8 mm and 10 mm, an average pore diameter of 2 μm) were kindly supplied from Nikkato. Corp., and were used as supports for the BTESE-derived membranes. Two types of α-Al_2O_3 particles (average size: 1.5 and 0.2 μm, Sumitomo Chemicals Inc.) were coated onto the outer surface of a porous support using a silica-zirconia colloidal sol (SiO_2−ZrO_2), which was prepared from tetraethoxysilane (TEOS) using zirconium tetrabutoxide as a binder, and was then fired at either 550 or 700 °C for 15 min to smooth the surface. Silica-zirconia colloidal sol diluted to 0.5 wt% was coated onto the substrate to form an intermediate layer with pore sizes of 1-2 nm, followed by firing at either 550 or 700 °C for 15 min. These procedures were repeated several times to cover the larger pores that might have resulted in pinholes in the separation layers. Finally, the BTESE-derived sols were coated onto the intermediate layer to

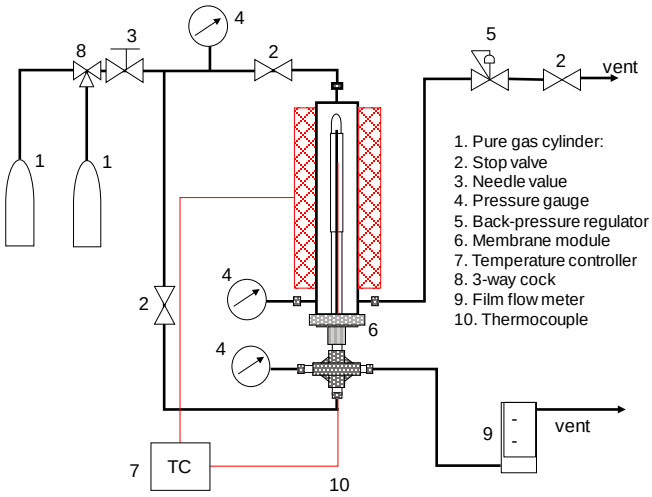

Figure. 1 A schematic diagram of the experimental apparatus for a single-gas permeation measurement.

serve as a separation layer, followed by drying and firing at 300, 550 and 700 °C under N_2 for 20 min. The coating and firing of the BTESE-derived sols was repeated 3-4 times.

Single-gas permeation measurement

Figure 1 displays a schematic diagram of the experimental apparatus for a single-gas permeation measurement. The gas permeation tests were carried out at 50−550 °C and controlled with a thermocouple inside the membrane. He, H_2, CO_2, N_2, CH_4, C_3H_8, CF_4, and SF_6 were fed to the outside (upstream) of a cylindrical membrane with a trans-membrane pressure of 0.1−0.2 MPa that was controlled with a back-pressure regulator, while the permeate stream was maintained at atmospheric pressure. Membranes were heated to 500 and 550 °C under N_2 and then under air to evaluate the thermal stability and oxidative resistance, and then the permeances for N_2 and for a series of gases were measured after cooling to 300 °C to monitor the pore size distribution. The temperatures were increased at a heating rate of 5 °C/min and decreased naturally with membrane heating under a transmembrane pressure of 0.1 MPa for the feed side using N_2. The gas flow rate through the membrane was measured using a bubble film flow meter (SF-U, Horiba, Co. Ltd., Japan).

Results and Discussion

Characterization of BTESE-derived gel

Figure 2 shows the ATR FT-IR spectra of the BTESE powders fired at 100, 200, 300, 550, and 700°C, which hereafter will be referred to P100, P200, P300, P550, and P700, respectively. P100, P200, and P300 showed absorption peaks for Si-C_2H_4-Si groups at locations approximately consistent with the spectrum reported for BTESE-derived powders: 690, 1160, 1270, 1410 and 2890 cm^{-1}.[18, 37, 38] With an increase in the firing temperatures from 100 to 550 °C, the peaks originating from Si-C_2H_4-Si linking units decreased significantly,[33] ethane groups observed at approximately 1270 and 1410 cm^{-1} were decomposed, and hydrogen was released (as will be discussed in Fig. 3b). On the other hand, new peaks were clearly observed at around

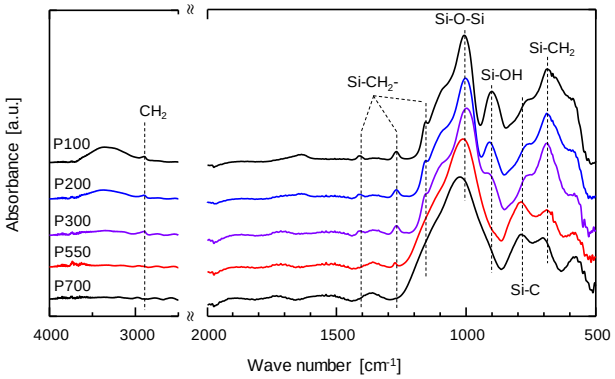

Figure 2. FT-IR spectra of BTESE powders fired under N_2 from 100 to 700 °C. P100−700 were powders fired at 100−700 °C under N_2, respectively.

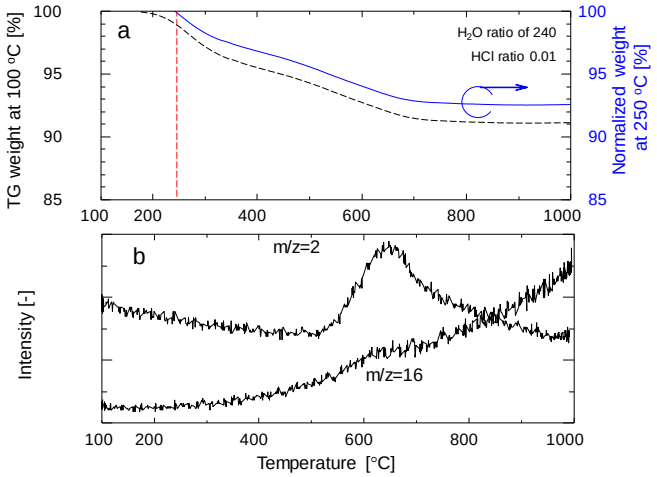

Figure 3. (a) Thermogravimetric weight of BTESE-derived powders under N_2 with a ramping rate of 10 °C/min. (Dotted and solid curves show TG weight normalized at 100 and 250°C, respectively) (b) The mass signal (m/z) for powders fired under N_2.

800 cm^{-1}, which can be assigned to the stretching of Si-C. When the pyrolysis temperature was further raised beyond 700 °C, nearly all the ethane disappeared; only the peaks of Si-O-Si and Si-C were observed, suggesting the formation of a network of either Si-O-C[39] and/or SiC[37] via the dehydrogenation, decomposition and rearrangement of linking units, Si-CH_2CH_2-Si and siloxane SiOSi. Si-OH groups observed at 900 cm^{-1} for P100, P200 and P300, were diminished for P500 and P700, due to condensation of the Si-OH groups to form Si-O-Si when firing temperatures were higher than 300 °C, suggesting that the BTESE network became denser at high temperatures. Figure 3a exhibits the TG weight and mass signal (m/z) of BTESE powders calcinated under N_2 from 100 to 1000 °C. To prepare pH-swing sols, NH_4Cl was synthesized during a pH swing from acid (HCl) to alkali via the addition of NH_3, which was followed by another swing back to acid that indicated the dried gels contained NH_4Cl. In our previous work, we confirmed that pH swing powders (H^+ ratio of 0.1) showed a weight loss at 200 °C, which could be ascribed to the decomposition of NH_4Cl[30] that was completed at 250 °C (Supplementary information, SI-1). In the present study, the normalized weight at 250 °C was used to eliminate the effects of

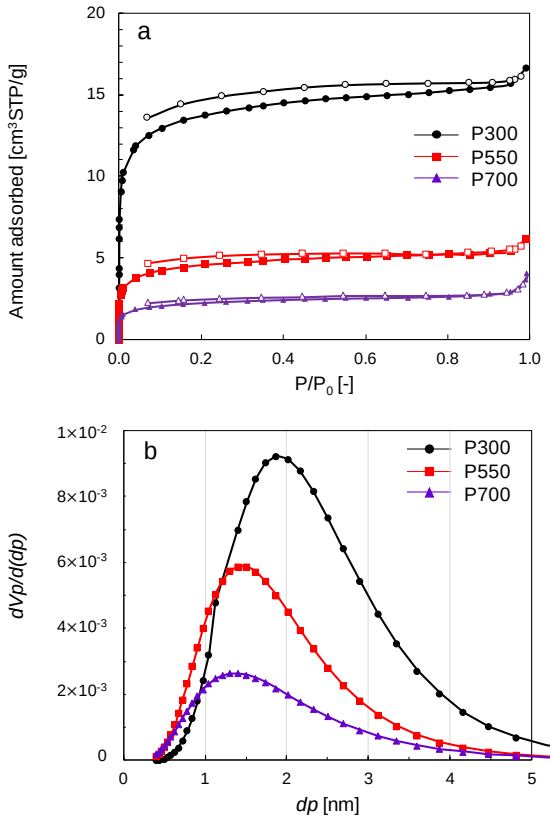

Figure 4. (a) N_2 adsorption (closed keys)/desorption (open keys) isotherms at 77 K and (b) pore size distribution for BTESE powders fired at different temperatures under N_2.

Table 1. The BET areas and pore volumes (V_p) of BTESE powders fired at different temperatures under N_2.

BTESE powders	BET surface area (m^2/g)	V_p (cm^3/g)
P300	55.8	0.1360
P550	16.6	0.0694
P700	8.0	0.0277

NH_4Cl, as shown by the solid blue curve in Figure 3a. The residual weight of BTESE powders was decreased at temperatures that ranged from 250 to 1000 °C, which corresponded to the dehydroxylation of Si-OH groups at 250-400 °C and to the partial pyrolysis of Si-CH_2CH_2-Si linking units, and was accompanied by cleavage and rearrangement at 400-700 °C.[41] Figure 3b shows the mass peaks (m/z=2, 16) that correspond to H_2 and CH_4. The TG weight decrease due to the losses of hydrogen and carbon ranging from 550 to 700 °C, is consistent with the trend observed by FT-IR.

Figure 4a shows the N_2 adsorption/desorption isotherms at 77 K for P300, P550 and P700. The specific surface areas and pore volumes are listed in Table 1. The N_2 isotherms showed a Type 1 pattern that indicates the existence of micropores. The BET surface area of P300 was 55.8 m^2/g, which was relatively small compared with conventional acid-based sols since higher cross-linking was obtained via the pH-swing[30] at a lower value of acid ratio (0.01).[31, 34] The BET surface areas of P550 and P700 were decreased to 16.6 and 8.0 m^2/g, respectively, indicating an increase in the firing temperature, and the BET surface areas of BTESE-derived powders were decreased. Figure 4b shows the pore size distributions via the NLDFT method. With an increase in the firing temperature of from 300 to 700 °C, the pore-size distribution showed a maxima of 1.8 nm for P300 and a maxima of 1.3 nm for P700, which indicates that pore sizes decrease under higher temperatures. This could be consistent with gas permeation properties; the selectivities of H_2/N_2 and H_2/CH_4, which will be discussed in the next section, were increased with an increase in the calcination temperature, although N_2 adsorption provides a pore distribution larger than the size of N_2. Accordingly, the pore volume was decreased as firing temperatures increased from 300 to 700 °C as presented in Table 1, suggesting the network structures were densified at high temperatures. The pore structures were characterized by N_2 adsorption, which confirmed that high temperature promoted the densification of BTES-derived networks induced by the condensation of Si-OH and the rearrangement of Si-CH_2CH_2-Si bonds to Si-O-Si and Si-C bonds, which was suggested via FT-IR and TG-MASS.

Gas permeation properties of BTESE membranes fired at 300, 500 and 700 °C

BTESE membranes were prepared by coating BTESE sols onto SiO_2-ZrO_2 intermediate layers and firing at 300, 550 and 700 °C, which hereafter are referred to as M300, M550 and M700, respectively. Values for the gas permeance of various molecules are plotted as a function of the kinetic diameter, as shown in Figure 5. The gas permeance of all three membranes showed a sharp dependence on kinetic diameter at 300 °C with H_2/CH_4 high selectivities of 60, 100, and 500 for M300, M550, and M700, respectively. Irrespective of firing temperatures, the membrane morphologies of BTESE-derived membranes were similar, and their permeation resistance was dominated by the separation layer (Supplementary Information SI-2). The M300 membrane showed a H_2 permeance that reached as high as 9.0×10^{-7} mol/(m^2 s Pa) with permeance ratios for H_2/CH_4 and H_2/C_3H_8 of 60 and 16,000, respectively. M550 showed H_2 permeance that was lower than that of M300, but higher than 6×10^{-7} mol/(m^2 s Pa), which corresponds to a GPU of 1,800. The H_2 permeance was larger than that of He (8.1×10^{-7} mol/(m^2 s Pa)) for M300, but the permeance of He (kinetic diameter: 0.26 nm) was larger than that of H_2 (kinetic diameter: 0.289 nm) for M700. In addition, the selectivity of H_2/N_2 was larger than 100 for M700, indicating that major parts of BTESE-derived membranes consisted of small pores that N_2 could not access. The smaller size of He resulted permeance larger than that of H_2 based on the molecular sieving when the pore sizes of the network were decreased at temperatures higher than 550 °C due to the rearrangement of Si-CC-Si linking units. By comparison with M550 and M300, the M700 membrane was more selective for H_2/CH_4, although the values of CF_4 and SF_6 permeance were higher for M700, which can be theoretically predicted via the gas-translation model reported by Gang Li et al.[41] This is because M700 retained bimodal structures consisting of small pores, which only small molecules such as He and H_2 could permeate, and large pores that allowed the permeation of He, H_2, and as well as large molecules such as CF_4, (Supplementary Information, SI-3). With preparation temperatures from 300 to 700 °C, the SiCCSi linking units underwent partial pyrolysis and a resultant rearrangement, but all membranes showed high selectivity and high H_2 permeance.

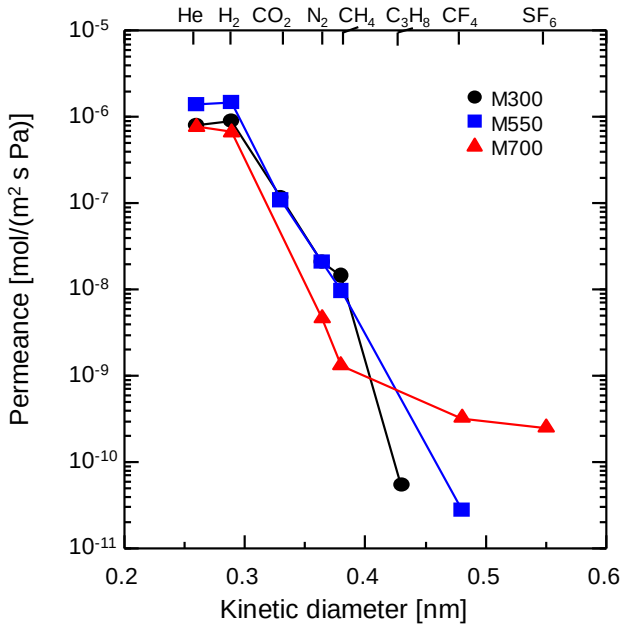

Figure 5. The relationship between gas permeance and kinetic diameter at 300 °C. The circle, square and triangle keys represent membranes fired at 300, 550 and 700 °C, respectively.

More than ten membranes were prepared to confirm the reproducibility and permeation properties of H_2 permeance, and He/H_2, H_2/CH_4, and H_2/N_2 selectivity against firing temperatures, as summarized in Figure 6. Each point corresponds to one BTESE-derived membrane. BTESE-derived membranes prepared by firing at 300, 500 and 700 °C showed H_2 permeance of 7.5–15×10^{-7}, 3.5–16×10^{-7}, and 5.4–7.2×10^{-7} mol/(m^2 s Pa), selectivity for H_2/CH_4 of 15–120, 80–390 and 290–920, and selectivity for H_2/N_2 of 16–60, 46–130, 140–350 with reasonable reproducibility, respectively, which indicated that H_2 permeance was decreased and the selectivities of He/H_2, H_2/N_2 and H_2/CH_4 were shifted to a higher level with an increase in firing temperatures. Figure 6b shows the selectivities for He/H_2, which are the most suitable for discussing the pore size of a network since the permeance of the two smallest molecules would be less affected than that of larger molecules such as CF_4 and SF_6 because of the existence of pinholes. The selectivities of He/H_2 were increased from near Knudsen selectivity (0.707) to values larger than 1 with an increase in the firing temperatures of from 300 to 700 °C. This is consistent with the results found by Qi et al., who prepared BTESE-derived membranes by firing at 400 and 600 °C.[33] Again, when the firing temperatures were lower than 550 °C, the permeance of H_2 (mole weight: 2 g/mol) was higher than that of He (MW: 4 g/mol), which showed Knudsen diffusion. Increasing the firing temperatures to 600 and 700 °C increased the permeance of He to a higher level than that of H_2 since the molecular size of He is smaller than that of H_2, confirming that the pore size of BTESE-derived membranes decreases with increases in firing temperatures.

Figure 7 summarizes the H_2/CH_4 permeance ratio as a function of H_2 permeance at 200–300 °C for BTESE, silica, and several types of zeolite and zeolitic imidazolate framework (ZIF) membranes. For the BTESE-derived membranes in this study, the average values for H_2 permeance were 1.0×10^{-6}, 9.4×10^{-7}, and 6.4×10^{-7} mol/(m^2 s Pa), and the averages permeance ratios of H_2/CH_4 were 57, 160 and 570 for membranes prepared at 300, 550 and 700 °C, respectively. Although the permeance of H_2 was slightly decreased, the higher preparation temperatures increased the selectivity of the BTESE membranes. It is noteworthy that, the performances of BTESE membranes in our work showed superior performances to zeolite and ZIF membranes, which may have been due to the pore sizes of those membranes being too

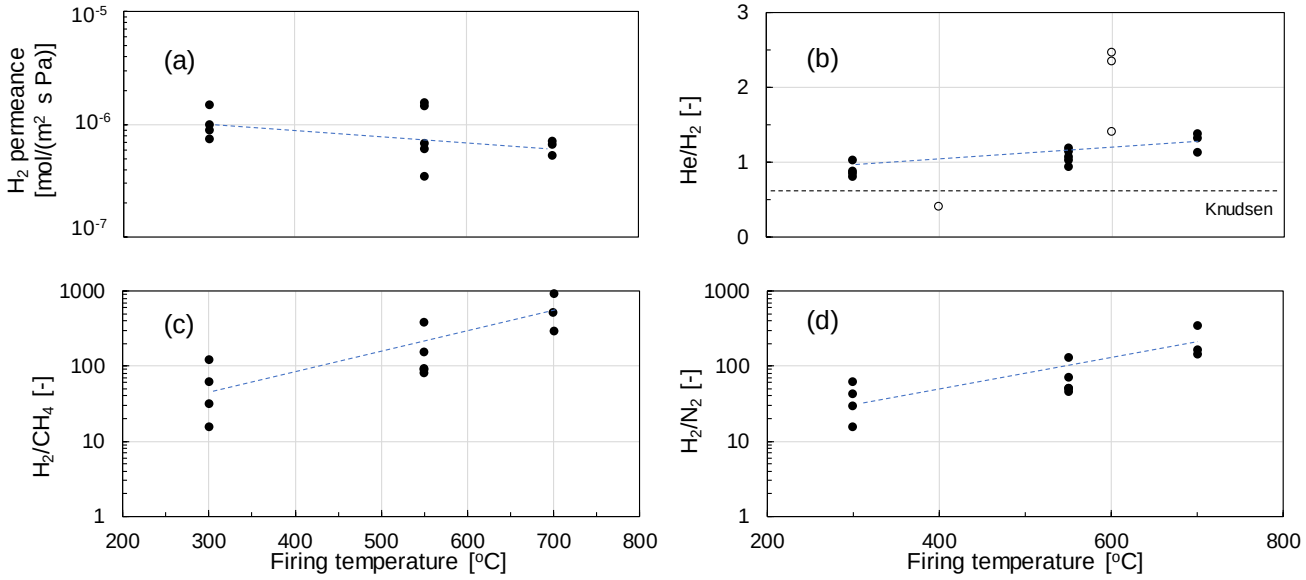

Figure 6. The relationship between firing temperatures and H_2 permeance (a) and selectivity of He/H_2 (b) (open keys are data from Qi group[33]), H_2/CH_4 (c) and H_2/N_2 (d). Gas permeance was measured at 300 (this work) and 200 °C (Qi group).

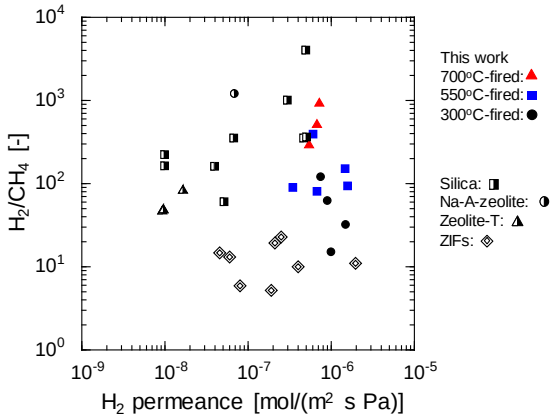

Figure 7. Trade-off plot of H_2/CH_4 selectivity versus H_2 permeance for membranes at 150−300 °C. For other membranes, data were taken from the literature (Silica[8, 9, 42-44], Na-A-zeolite[45], Zeolite-T[46], ZIFs[47-50]) and are summarized in the supplementary information (SI-4).

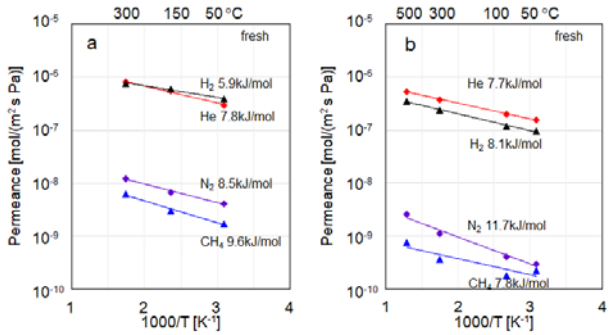

Figure 8. The temperature dependency of gas permeance for the BTESE-derived membranes. (a: fired at 300 °C. b: fired at 550 °C)

large for the purification of hydrogen. In addition, BTESE membranes fired at high temperatures showed lower selectivity and higher permeance compared with silica membranes. This is because the pore sizes of BTESE membranes were larger than those of the TEOS-derived membrane (0.36−0.38 nm).[9] By using the spacer methods mentioned in the Introduction section, the pore sizes of BTESE-derived membranes could be controlled by the size of the linking units between the two Si atoms. These results represent the first example of BTESE-derived membranes prepared with firing under high temperatures (500−700 °C) and showing high permeance with reasonable selectivity.

A modified gas translation model as expressed by Eq. (1) was used to describe the gas permeation properties through microporous membranes,[8, 33, 51, 52].

$$P_i = \frac{k_{0,i}}{\sqrt{M_i RT}} \exp\left(-\frac{E_{p,i}}{RT}\right) \qquad (1)$$

In Eq. (1), P_i, $k_{o,i}$, M_i and $E_{p,i}$ are the permeance, permeation constant, molecular weight and activation energy of permeation, respectively, for the ith component. R is the gas constant, and T is the absolute temperature.

Figure 8a and 8b shows the temperature dependency of BTESE membranes fired at 300 and 550 °C under N_2, respectively. The permeance of He, H_2, N_2, and CH_4 increased with increasing temperature, which showed an activated permeation mechanism. The activation energy (E_p), which reflected the difficulty of molecular permeation through membrane pores,[53] was obtained by fitting the temperature dependency of gas permeance with Eq. (1). The activation energy of H_2 permeation was slightly increased for membranes prepared from 300 to 700 °C, suggesting H_2 permeation through the densified networks had become restricted by molecular sieving. On the other hand, the activation energy of N_2 was larger than that of He and H_2 due to the larger size. N_2 activation energy increased from 8.5 to 11.7 kJ/mol with an increase in firing temperatures, which indicated the permeation of larger molecules had been hindered by the densification of Si-OH and Si-CH_2CH_2-Si at high temperatures. In temperatures ranging from 500 to 50 °C, the selectivities of H_2/N_2 and H_2/CH_4 were 140−320 and 400−650, respectively, suggesting that BTESE-derived membranes fired at temperatures as high as 550 °C under N_2 show promise for use in gas separation over a wide range of temperatures.

Stability of membranes at high temperature under an oxidation atmosphere

To further discuss the gas permeation properties, a BTESE membrane prepared at 300 °C was evaluated in terms of its stability under thermal and oxidative conditions over a long duration. This BTESE membrane was first tested continuously for more than 6 h at 500 °C and then at 550 °C under N_2. During heat treatment under N_2, as shown in Figure 9a, the permeance of N_2 was stable at 1.9×10^{-8} mol/(m² s Pa) at 300 °C for the first 2 h. With an increase in temperature, N_2 permeance increased gradually and then began to stabilize at around 5.6×10^{-8} mol/(m² s Pa) at 500 °C for 5 h, and 6.2×10^{-8} mol/(m² s Pa) at 550 °C for 10 h. N_2 permeance was measured at 300 °C to monitor the change in membrane performance from 1.9×10^{-8} mol/(m² s Pa) for the initial measurement to 5.6×10^{-8} mol/(m² s Pa) after 500 °C and to 6.2×10^{-8} mol/(m² s Pa) after 550 °C, which indicated that N_2 permeance had obviously increased following heat treatment under N_2. After cooling to 300 °C, the feed gas was switched to air, and then the temperature was increased from 300 to 550 °C. The air permeance increased from 4.0×10^{-8} mol/(m² s Pa) at 300 °C and reached a steady permeance of 2.5×10^{-7} mol/(m² s Pa) at 550 °C after 10h.

A similar long-term stability test was carried out on a BTESE membrane prepared at 550 °C (M500), as shown Figure 9b. During the first period of heat treatment at 300 to 500 °C, N_2 permeance was in-creased from 2.0×10^{-8} mol/(m² s Pa) to a maximum value of 3.6×10^{-8} mol/(m² s Pa) at the start of 500 °C treatment, and then the permeance decreased slightly and remained stable after 6 h. This may have been because the membrane showed activated diffusion when the temperature first reached 500 °C, but the network turned to a much denser structure due to the rearrangement of the Si-CC-Si units as suggested by FT-IR and BET analysis, which resulted in decreased permeance for an extended period of time at 500 °C. The initial N_2 permeance measured at 300 °C was 2.0×10^{-8}, and was 3.6×10^{-8} when the temperature was raised to 500 °C, and then 3.7×10^{-8} mol/(m² s Pa) at 550 °C, indicating N_2 permeance was stable irrespective of long-term heat treatment. This is because this

membrane was prepared by firing at 550 °C for more than 90 min, which induced sufficient condensation of Si-OH and/or rearrangement of the Si-CC-Si networks during the membrane calcination. After changing the feed gas from N_2 to air and increasing the temperature from 300 to 550 °C, air permeance increased from 2.6×10^{-8} to 1.6×10^{-7} mol/(m^2 s Pa), which might be ascribed to the oxidation of carbon and to the loose networks, as illustrated in Figure 9.

The permeance of gas molecules with various kinetic diameters was measured at 300 °C following each heat-treatment step, as summarized in Figure 10a. A fresh M300 membrane held selectivity for H_2/C_3H_8 that exceeded 10^4 with a H_2 permeance of approximately 10^{-6} mol/(m^2 s Pa). After air treatment at 550 °C, the permeance for all gases increased drastically; for example, the fresh-membrane permeance of H_2 increased more than three-fold to 2.9×10^{-6} mol/(m^2 s Pa). On the other hand, such heat-treated membranes lost their original levels of permselectivity after 8 h of air treatment at 550 °C, which ultimately reduced the selectivity for H_2/CH_4 from 61 to 23, and the selectivity for H_2/CF_4 fell from >10^4 to 320. This decrease in membrane selectivity can be ascribed to a decomposition of the organic linking units via oxidation. Figure 10b illustrates the impact of oxidation under air at 550 °C on an M550 membrane; H_2 permeance was slightly increased but selectivity of H_2/CH_4 remained at 140. The H_2 and N_2 permeance values of the M550 were increased to 2.7×10^{-6} and 1.3×10^{-7} mol/(m^2 s Pa) with H_2/CF_4 and N_2/CF_4 selectivities of 1200 and 60, respectively. Following air treatment for M700 membrane, the permeance for H_2 and N_2 were increased to 1.6×10^{-6} and 8.2×10^{-8} mol/(m^2 s Pa), respectively, while the selectivities for H_2/CF_4 and N_2/CF_4 were maintained at 1600 and 80, respectively. The M550 and M700 BTESE membranes showed a much higher level of selectivity for H_2/CF_4 than that of M300, which certified the high separation ability of these membranes even after 550 °C air treatment irrespective of Si-CC-Si units that may decompose under air. This higher level of selectivity was due to enhanced levels of thermal stability and oxidative resistance.

Figure 11 shows H_2/CH_4 selectivity as a function of H_2 permeance for BTESE membranes fired at 300, 550 and 700 °C and treated under air at 550 °C for 8 h. Similar to the fresh membranes shown in Figure 7, H_2 permeance for M300, M550 and M700 was approximately the same. On the other hand, after air treatment, obviously, the H_2/CH_4 selectivity levels of M550 and M700 were much higher than that of M300. The higher permeance ratios of M550 and M700, compared with that of M300, were the result of selectivity that was higher under fresh conditions and a CH_4 permeance that increased less after

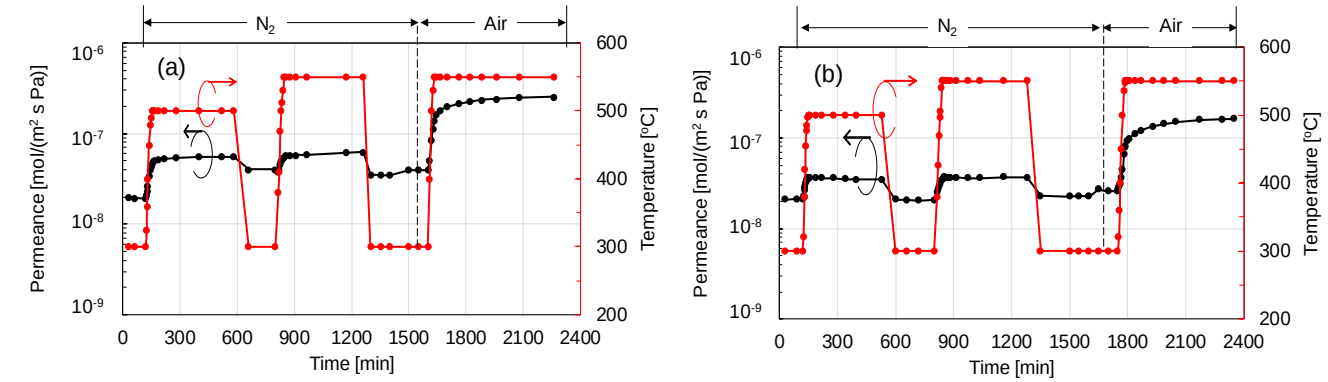

Figure 9. The time course of N_2 and air permeance with heat treatment for BTESE-derived membranes prepared at 300 (a) and 550 °C (b).

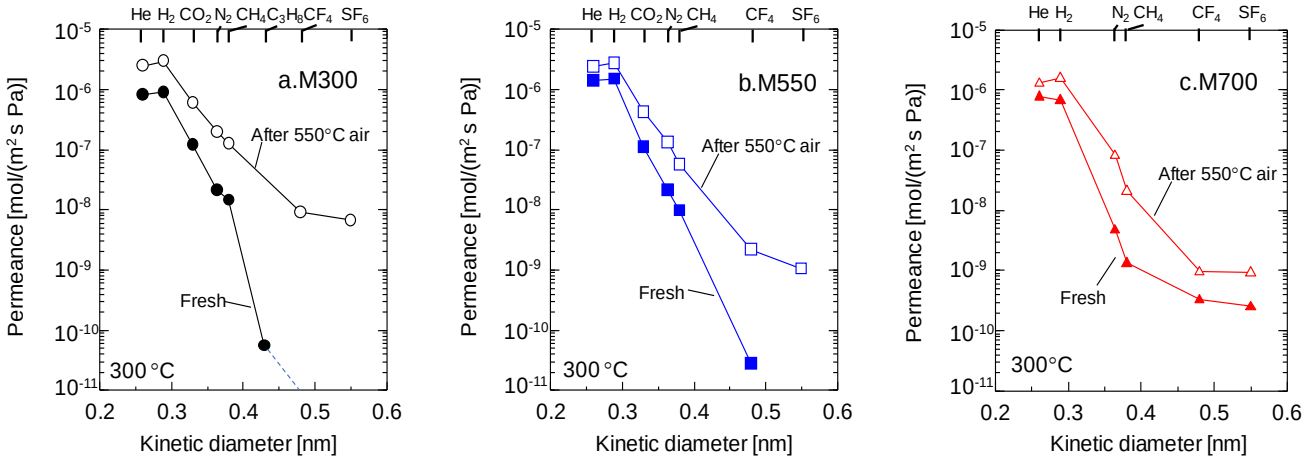

Figure 10. The relationship between the kinetic size of gas molecules and gas permeance at 300 °C for a fresh membrane and following air treatment at 550 °C. Membranes prepared at 300, 550 and 700 °C appear in (a), (b) and (c), respectively.

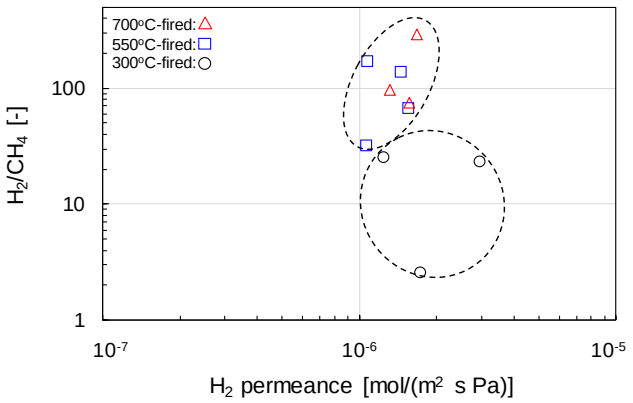

Figure 11. H_2/CH_4 selectivity as a function of the H_2 permeance of BTESE membranes after firing under air at 550 °C. Membranes prepared at 300, 550 and 700 °C are highlighted by the circle, square and triangle keys, respectively.

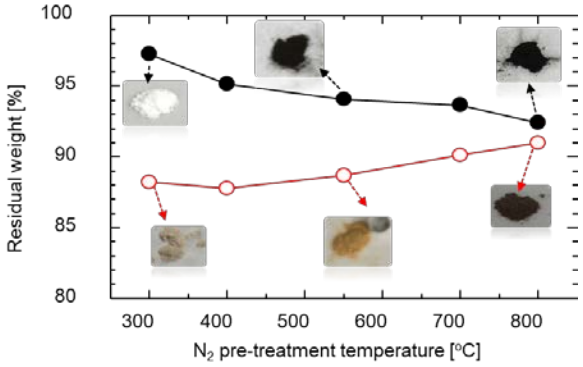

Figure 12. Residual weight of BTESE-derived powders fired under N_2 (closed keys) and air at 600 °C after N_2-pretreatment (open keys) as a function of N_2-preatment temperatures. The photos show powders after TG analysis.

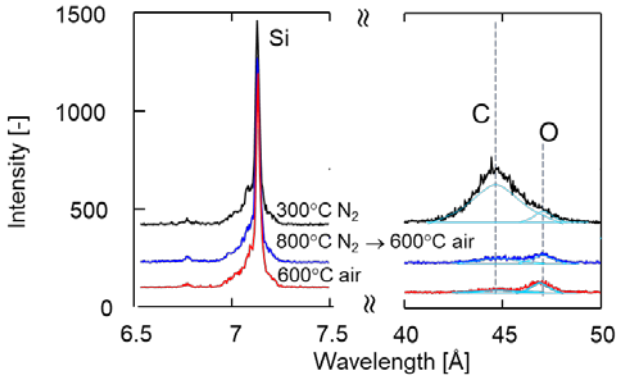

Figure 13. Spectra of C, O and Si element detected in BTESE particles.

air treatment. This demonstrates how BTESE membranes prepared at high temperatures were more thermally stable under both N_2 and air, which shows promise for gas separation at high temperature even under an oxidizing atmosphere.

The thermal stability and oxidative resistance of BTESE-derived powders prepared under N_2 at 300, 400, 550, and 800 °C, which will be referred as P300, P400, P550, and P800, respectively. Each was investigated by thermogravimetric (TG) analysis to clarify the effect of firing temperatures. In the first step, the residual weight of powders was measured at 250 °C before and after heat treatment under N_2 at different temperatures from 300 to 800 °C, as shown by the closed keys in Figure 12. Increases in temperature clearly showed a decreasing trend, which can be ascribed to the decomposition of hydrocarbon linking groups, as mentioned in FT-IR. In the next step, after pretreatment at 300–800 °C under N_2, powders received further heat treatment under air at 600 °C for 2 h (open keys). The TG weight of the powders was decreased by the oxidation of non-decomposed -CH- groups during N_2 pretreatment. The P300 powder showed a weight reduction from 97.3% (after firing under N_2 at 300 °C) to 88.2% (after firing under air at 600 °C), which was a weight loss of approximately 9%. With increases in temperature under N_2 pre-treatment, reductions in weight loss of 3.5% and 1.3% were observed for P700 and P800, respectively. After the N_2 pre-treatment, P550 and P800 had a dark color, which suggests that a certain amount of carbon remained. After treatment at 600 °C under air, the P300 powder turned slightly yellow and the color of the P550 powder turned from black to yellowish, suggesting that some amount of carbon had been oxidized. The color of the P800 powder following treatment at 600 °C under air remained deep brown, which suggests a larger amount of carbon remained. In addition, the residual weight of the BTESE powders after treatment at 600 °C under air was increased from 88.2% (P300) to 91.0% (P800), which was probably related to a higher degree of condensation and indicated a stabilized organosilica network was achieved by the thermal rearrangement of Si-CH_2CH_2-Si and Si-O-Si.

Powders after firing under N_2 and air at different temperatures were analyzed via EPMA measurement, as shown in Figure 13. Silicon, carbon and oxygen are represented by the wavelengths at 0.72, 0.44, and 0.47 nm, and these chemical compositions are summarized in Table 2. The C/Si ratio was 1.15 for powders fired under N_2 at 300 °C, which approximates a theoretical value of 1. The C/Si ratio was decreased to 0.56 for P800. The existence of large amounts of carbon was confirmed even for BTESE powders treated at 300–800 °C under N_2, suggesting that the residual carbon made a significant contribution to the formation of dense networks that larger sized molecules have trouble permeating. This phenomenon was previously discussed for M550 and M700, which showed high H_2/CH_4 selectivity under fresh conditions. In other words, the highest level of selectivity recorded by the M700 membrane can be ascribed to a higher C/Si ratio, which suggests that the Si-CH_2CH_2-Si linking units were changed to densified networks consisting of Si-C and Si-O-Si structures. When BTESE powder was directly treated at 600 °C under air, carbon was decreased drastically to a C/Si ratio of 0.09, which accounts for the drastically increased gas permeance and decreased selectivity for BTESE membranes fired at 300 °C under N_2 after treatment under air. The dense network was loosened because most of the organic linking units were oxidized. On the other hand, following pre-treatment (N_2 treatment) at 600 °C with subsequent firing under air at 600 °C, the C/Si ratio remained at 0.15, which was higher than that of powders fired directly under air at 600 °C. The

C/Si ratio was increased from 0.15 to 0.23 for powders pretreated at 600 and 800 °C under N_2, which indicates that networks more stable against oxidative conditions were formed by firing at higher temperatures under N_2. After air treatment at 600 °C, the values for the gas permeance of M550 and M700 were stable compared with that of M300, which is consistent with the results of BTESE-derived powders, and indicates that Si-C forms networks that are highly stable to thermal conditions through pyrolysis and rearrangement by firing at 550 and 700 °C. This demonstrates that high-temperature N_2 treatment increases the thermal and oxidation stability of BTESE-derived organosilica membranes.

Table 2. Chemical composition (mol%) of Si, C and O determined by EPMA.

Treatment	Si%	C%	O%	C/Si ratio
300 °C N_2	25.5	29.4	45.1	1.15
600 °C N_2	28.7	22.5	48.8	0.78
800 °C N_2	30.1	17.0	52.9	0.56
600 °C air	33.9	3.1	63.0	0.09
600 °C N_2 → 600 °C air	31.2	4.8	64.0	0.15
800 °C N_2 → 600 °C air	27.9	6.4	65.7	0.23

Conclusions

Defect-free BTESE membranes were prepared at 300, 550, and 700 °C under N_2. These membranes exhibited molecular sieve permeation properties (H_2/CH_4>100, H_2/CF_4>2000) with H_2 permeance of approximately 10^{-6} mol/(m^2 s Pa). Compared with BTESE membranes prepared at 300 °C, the selectivity for H_2/CH_4 of 700 °C-fired membranes was higher, reaching a value of 570 with H_2 permeance of approximately 10^{-6} mol/(m^2 s Pa). Moreover, even after heat treatment at 550 °C under N_2 followed by treatment under air, these BTESE-derived membranes retained levels of selectivity for H_2/CH_4 and H_2/CF_4 that reached as high as 100 and 2,000, respectively, while the selectivity for H_2/CH_4 and H_2/CF_4 of membranes prepared at 300 °C only reached 30 and 200, respectively. A larger carbon/silicon ratio (approximately 0.2) resulted in the formation of Si-C, and the residual weight remained high for powders with multiple heat treatments under N_2 followed by treatment under air, which suggested that the thermal stability and oxidizing resistance was increased for these BTESE-derived membranes prepared at high temperatures under N_2. In addition, these BTESE-derived membranes prepared under high temperatures showed excellent selectivity with high levels of H_2 permeance and a permeation performance that could be tailored by treatment under air at 550 °C for as long as 10 h.

Conflicts of interest

There are no conflicts to declare.

Acknowledgements

This work was supported by the Cross-ministerial Strategic Innovation Promotion Program (SIP) of the Energy Carrier Project of the Japan Science and Technology Agency (JST) and the Japan Society for the Promotion of Science (JSPS) KAKENHI Grant Number JP17J00447.

Notes and references

1. W. J. Koros and C. Zhang, *Nat. Mater.*, 2017, **16**, 289-297.
2. G. Li, T. Niimi, M. Kanezashi, T. Yoshioka and T. Tsuru, *Int. J. Hydrogen Energy*, 2013, **38**, 15302-15306.
3. F. C. Gielens, R. J. J. Knibbeler, P. F. J. Duysinx, H. D. Tong, M. A. G. Vorstman and J. T. F. Keurentjes, *J. Membr. Sci.*, 2006, **279**, 176-185.
4. H. J. Alves, C. Bley Junior, R. R. Niklevicz, E. P. Frigo, M. S. Frigo and C. H. Coimbra-Araújo, *Int. J. Hydrogen Energy*, 2013, **38**, 5215-5225.
5. C. E. Powell and G. G. Qiao, *J. Membr. Sci.*, 2006, **279**, 1-49.
6. M. K. Mondal, H. K. Balsora and P. Varshney, *Energy*, 2012, **46**, 431-441.
7. H. B. Park, J. Kamcev, L. M. Robeson, M. Elimelech and B. D. Freeman, *Science*, 2017, **356**.
8. M. Kanezashi, T. Sasaki, H. Tawarayama, H. Nagasawa, T. Yoshioka, K. Ito and T. Tsuru, *J. Phys. Chem. C*, 2014, **118**, 20323-20331.
9. Renate. M. d. Vos and H. Verweij, *Science*, 1998, **279**, 1710–1171.
10. Renate M. de Vos, Wilhelm F. Maier and H. Verweij, *J. Membr. Sci.*, 1999, **158**, 277-288.
11. H. Song, S. Zhao, J. Chen and H. Qi, *Microporous Mesoporous Mater.*, 2016, **224**, 277-284.
12. V. Boffa, D. Blank and J. Tenelshof, *J. Membr. Sci.*, 2008, **319**, 256-263.
13. G. P. Fotou, Y. S. Lin and S. E. Pratsinis, *J. Mater. Sci.*, 1995, **30**, 2803-2808.
14. H. L. Castricum, R. Kreiter, H. M. van Veen, D. H. A. Blank, J. F. Vente and J. E. ten Elshof, *J. Membr. Sci.*, 2008, **324**, 111-118.
15. M. Kanezashi, K. Yada, T. Yoshioka and T. Tsuru, *J. Am. Chem. Soc.*, 2009, 414-415.
16. X. Ren, M. Kanezashi, H. Nagasawa and T. Tsuru, *J. Membr. Sci.*, 2015, **496**, 156-164.
17. H. L. Castricum, G. G. Paradis, M. C. Mittelmeijer-Hazeleger, R. Kreiter, J. F. Vente and J. E. ten Elshof, *Adv. Funct. Mater.*, 2011, **21**, 2319-2329.
18. T. Niimi, H. Nagasawa, M. Kanezashi, T. Yoshioka, K. Ito and T. Tsuru, *J. Membr. Sci.*, 2014, **455**, 375-383.
19. H. Marcel ten, A. Nijmeijer and L. Winnubst, *Sep. Purif. Technol.*, 2015, **147**, 372-378.
20. H. Qi, J. Han and N. Xu, *J. Membr. Sci.*, 2011, **382**, 231-237.
21. H. L. Castricum, H. F. Qureshi, A. Nijmeijer and L. Winnubst, *J. Membr. Sci.*, 2015, **488**, 121-128.
22. X. Yang, H. Du, Y. Lin, L. Song, Y. Zhang, X. Gao, C. Kong and L. Chen, *J. Membr. Sci.*, 2016, **506**, 31-37.
23. G. Li, M. Kanezashi, T. Yoshioka and T. Tsuru, *AIChE J.*, 2013, **59**, 168-179.
24. L. Meng, X. Yu, T. Niimi, H. Nagasawa, M. Kanezashi, T. Yoshioka and T. Tsuru, *AIChE J.*, 2015, **61**, 1628-1638.
25. R. Xu, J. Wang, M. Kanezashi, T. Yoshioka and T. Tsuru, *AIChE J.*, 2013, **59**, 1298-1307.
26. S. M. Ibrahim, H. Nagasawa, M. Kanezashi and T. Tsuru, *J. Membr. Sci.*, 2015, **493**, 515-523.

27. G. Gong, J. Wang, H. Nagasawa, M. Kanezashi, T. Yoshioka and T. Tsuru, *J. Membr. Sci.*, 2014, **464**, 140-148.
28. H. Nagasawa, N. Matsuda, M. Kanezashi, T. Yoshioka and T. Tsuru, *J. Membr. Sci.*, 2016, **498**, 336-344.
29. H. F. Qureshi, A. Nijmeijer and L. Winnubst, *J. Membr. Sci.*, 2013, **446**, 19-25.
30. X. Yu, L. Meng, T. Niimi, H. Nagasawa, M. Kanezashi, T. Yoshioka and T. Tsuru, *J. Membr. Sci.*, 2016, **511**, 219-227.
31. N. Moriyama, H. Nagasawa, M. Kanezashi, K. Ito and T. Tsuru, *J. Sol-Gel Sci. Technol.*, 2018, **86**, 63-72.
32. J. Wang, M. Kanezashi, T. Yoshioka and T. Tsuru, *J. Membr. Sci.*, 2012, **415-416**, 810-815.
33. H. Song, Y. Wei and H. Qi, *J. Mater. Chem. A*, 2017, **5**, 24657-24666.
34. H. L. Castricum, G. G. Paradis, M. C. Mittelmeijer-Hazeleger, W. Bras, G. Eeckhaut, J. F. Vente, G. Rothenberg and J. E. ten Elshof, *Microporous Mesoporous Mater.*, 2014, **185**, 224-234.
35. J. Wang, G. Gong, M. Kanezashi, T. Yoshioka, K. Ito and T. Tsuru, *J. Membr. Sci.*, 2013, **441**, 120-128.
36. A. P. Dral, E. R. H. van Eck, L. Winnubst and J. E. ten Elshof, *J. Membr. Sci.*, 2018, **548**, 157-164.
37. Q. L. Hue, R. Taylor, R. J. Day and F. Heatley, *J. Mater. Sci.*, 2001, **36**, 4037-4043.
38. Mahendra S. K, Suresh P. K, Aail R. K and A. D. P., *Asian Journal of Pharmaceutical and Clinical Research*, 2015, **8**, 110-125.
39. K. Yamamoto, J. Ohshita, T. Mizumo and T. Tsuru, *J. Non-Cryst. Solids*, 2015, **408**, 137-141.
40. E. J. Kappert, H. J. Bouwmeester, N. E. Benes and A. Nijmeijer, *J. Phys. Chem. B*, 2014, **118**, 5270-5277.
41. G. Li, H. R. Lee, H. Nagasawa, M. Kanezashi, T. Yoshioka and T. Tsuru, *AIChE J.*, 2015, **61**, 2268-2279.
42. J.C. Diniz da Costa, G.Q. Lu, V. Rudolph and Y. S. Lin, *J. Membr. Sci.*, 2002, **198**, 9-21.
43. M. W. J. Luiten, N. E. Benes, C. Huiskes, H. Kruidhof and A. Nijmeijer, *J. Membr. Sci.*, 2010, **348**, 1-5.
44. H. Lim, Y. Gu and S. T. Oyama, *J. Membr. Sci.*, 2010, **351**, 149-159.
45. N. Nishiyama, M. Yamaguchi, T. Katayama, Y. Hirota, M. Miyamoto, Y. Egashira, K. Ueyama, K. Nakanishi, T. Ohta, A. Mizusawa and T. Satoh, *J. Membr. Sci.*, 2007, **306**, 349-354.
46. Y. Cui, H. Kita and K.-i. Okamoto, *J. Mater. Chem.*, 2004, **14**, 924.
47. Y. Li, F. Liang, H. Bux, W. Yang and J. Caro, *J. Membr. Sci.*, 2010, **354**, 48-54.
48. Y. S. Li, F. Y. Liang, H. Bux, A. Feldhoff, W. S. Yang and J. Caro, *Angew Chem Int Ed Engl*, 2010, **49**, 548-551.
49. J. Kim and D. Lee, *J. Mater. Chem. A*, 2016, **4**, 5205-5215.
50. A. Jomekian, R. M. Behbahani, T. Mohammadi and A. Kargari, *Microporous Mesoporous Mater.*, 2016, **234**, 43-54.
51. T. Yoshioka, M. Kanezashi and T. Tsuru, *AIChE J.*, 2013, **59**, 2179-2194.
52. H. Nagasawa, T. Niimi, M. Kanezashi, T. Yoshioka and T. Tsuru, *AIChE J.*, 2014, **60**, 4199-4210.
53. P. Hacarlioglu, D. Lee, G. V. Gibbs and S. T. Oyama, *J. Membr. Sci.*, 2008, **313**, 277-283.